PNAS RESEARCH ARTICLE | ECOLOGY

High functional vulnerability across the world's deep-sea hydrothermal vent communities

Joan M. Alfaro-Lucas[a,1,2], Abbie S. A. Chapman[b,1,2], Verena Tunnicliffe[a,c], and Amanda E. Bates[a]

Edited by Jody Deming, University of Washington, Seattle, WA; received February 23, 2024; accepted August 5, 2024

At the nearly pristine hydrothermal vents of the deep sea, highly endemic animals depend upon bacteria nourished by hydrothermal fluids that emerge as outflows from the seafloor. These animals are remarkable in tolerating extreme conditions, including high heat, toxic reduced sulfide, and low oxygen. Here, we test whether the extreme vent environment has selected for functionally similar species across the world's deep ocean, despite well-established global geographic patterns of high phylogenetic distinctness. High functional redundancy in species pools within regions suggests that the extreme environments select for species with specific traits. Yet, some regions emerge as functional hotspots where species pools with distinct functional trait compositions may represent geological idiosyncrasies of the habitats. Moreover, many species are functionally unique, an outcome of low species richness in a system where the species pool is small at all scales. Given the high proportion of functionally unique species, simulated species extinctions indicate that species losses would rapidly translate to the elimination of functionally irreplaceable species and could tip vent systems to functional collapse. Ocean changes and human-induced threats are expected to significantly impact many vent species as human activities expand in the remote deep sea. The opportunity exists now to take precautionary actions to limit the rates of extinction now ubiquitous in more accessible areas of Earth.

macroecology | functional biogeography | community assembly | functional diversity | functional resilience

Significance

Little is known about the functional biogeography and diversity of the animal communities inhabiting hydrothermal vent habitats in the remote deep ocean. Our global analysis of >500 vent species found that regional species pools can be very different in terms of the traits represented, likely due to geological setting and evolutionary history. Moreover, half of the global vent species are functionally unique, and our simulations suggest that potential species loss could quickly translate into functional loss across vent regions. In the current context of deep-sea exploitation and industrialization, proactive and aggressive measures are necessary to safeguard iconic hydrothermal vent communities.

Deep-sea hot springs, or hydrothermal vents, are small island-like habitats patchily distributed (10s to100s km) along the world's tectonic plate boundaries that contrast radically with the stable, energy-poor "background" environments of the deep sea (1). Vent habitats provide some of the harshest conditions for animal life on Earth with highly fluctuating, steep gradients of temperature (from >300 °C to cold, ambient seawater temperatures), heavy metals, and toxic, chemically reduced compounds (e.g., H_2S) (2, 3). Yet, reduced compounds support high in situ microbial chemoautolithotrophic production (4) that sustains dense communities of endemic, highly specialized animals that mainly disperse at larval stages from vent to vent (5, 6).

Deep-sea vent communities are one of the last frontiers on Earth where biodiversity has, to date, been minimally impacted by human activities (7, 8). Thus, hydrothermal vent systems present an extreme environmental setting with communities that have not yet shifted from historical baselines, offering a model system for determining fundamental ecological patterns and testing hypotheses (9). Similar environmental filters are expected to select for species that share common traits, leading to convergence across species occupying similar habitats but arising through different evolutionary lineages. Indeed, trait convergence of species from different regions but similar habitats occur in plants (10, 11), beetles (12), lizards (13), terrestrial mammals (14–16), and fishes (17–19).

At hydrothermal vents, environmental constraints posed by high temperature and toxic compounds may also filter for specific biological traits. For instance, species that host chemoautotrophic symbiotic bacteria, internally or on their body surfaces, are adapted to access reduced compounds and oxygen to provision their symbionts while dealing with the harsh and extreme fluctuations of the environment (20). The giant tubeworm *Riftia pachyptila*, for example, is an iconic vent species, found at the East Pacific Rise and Galápagos vents (hereafter East Pacific vents; *SI Appendix*, Fig. S1), that hosts chemoautotrophic bacteria internally in a specialized organ called the trophosome (21). The adaptations of vent species with feeding strategies other than chemosymbiosis may also converge given the high and focused productivity and the unique nature and constraints of vent habitats compared to the rest of the deep sea.

Taken together, the harsh environmental fluids, high productivity, and the island-like nature of vent habitats presumably create strong pressures that select for specific traits and

Author affiliations: [a]Department of Biology, University of Victoria, Victoria, BC V8P 5C2, Canada; [b]Centre for Biodiversity and Environment Research, Department of Genetics, Evolution and Environment, University College London, London WC1H 0NN, United Kingdom; and [c]School of Earth & Ocean Sciences, University of Victoria, Victoria, BC V8P 5C2, Canada

---

Author contributions: J.M.A.-L., A.S.A.C., and A.E.B. designed research; J.M.A.-L., A.S.A.C., and A.E.B. conceived the project; J.M.A.-L., A.S.A.C., V.T., and A.E.B. contributed the data; J.M.A.-L. performed the statistical analyses; J.M.A.-L. created the visualizations; J.M.A.-L. wrote the original draft of the manuscript; A.E.B. acquired the funding for the project; J.M.A.-L., A.S.A.C., V.T., and A.E.B. edited the final draft; J.M.A.-L., A.S.A.C., V.T., and A.E.B. reviewed the final draft; and J.M.A.-L., A.S.A.C., V.T., and A.E.B. wrote the final draft.

The authors declare no competing interest.

This article is a PNAS Direct Submission.

[1] To whom correspondence may be addressed. Email: jmalfarolucas@gmail.com or abbie.chapman@ucl.ac.uk.

[2] J.M.A.-L. and A.S.A.C. contributed equally to this work.

This article contains supporting information online at https://www.pnas.org/lookup/suppl/doi:10.1073/pnas.2403899121/-/DCSupplemental.

species that perform similar ecological roles, leading to trait convergence across regional species pools and high functional redundancy. However, evolutionary history can also constrain the emergence of traits across phylogenetic lineages and the set of ecological strategies that are possible for some taxa (22–24). Indeed, species composition at vents from different regions that have been phylo-geographically isolated differs as much as tropical and boreal forests (25). Consequently, unique sets of trait combinations possessed by only one or a few species in a community/region may occur, representing idiosyncratic evolutionary histories of different vent regions.

Here, we quantify different dimensions of the functional diversity of 511 species from 11 deep-sea hydrothermal vent regions identified in the world's deep ocean to investigate the functional convergence and uniqueness of vent ecosystems. Building from the sFDvent database (26), we include species across several orders of magnitude in size, inhabiting areas from under vigorous vent fluid influence to vent periphery, and from recently explored regions including vents of the Antarctic (27), Arctic (28), and SW Indian (29) oceans (*SI Appendix*, Fig. S1). We update six species traits capturing the performance of vent species and their influence on ecosystem processes: adult mobility, maximum body size, feeding mode, habitat complexity provided, chemosynthesis obligate (i.e., species occurring exclusively at vents, shared with other chemosynthesis-based habitats or non-chemosynthetic habitats), and zonation from vents (i.e., species inhabiting areas of high, medium, or low hydrothermal fluid influence).

First, to find functional axes determining typical species ecological strategies and to assess how vent environments constrain the diversity and combination of species traits, we created a global functional space. Species distributed across this functional space based on their functional dissimilarity. We then tested whether regional species pools share similar trait composition despite distinct taxonomic faunal compositions. We also tested whether regional species pools show similar trait diversity (functional dispersion) and high redundancy. We then focused on species functional uniqueness within regional pools, to quantify whether species with unique ecological strategies are rare, before simulating species extinctions to quantify their impacts on regional functional diversity. We designed null models to disentangle the values of observed functional responses from changes expected solely due to species richness differences.

Results and Discussion

The successful ecological strategies of hydrothermal vent species are constrained to a small set of trait combinations distributed mainly along two independent functional axes related to life-history traits and habitat specialization (Fig. 1). The 511 species represent 167 unique trait combinations, as determined by the possible combinations across trait categories, of a total potential of 3,456 combinations (<5%) suggesting that most potential trait combinations are not realized in this set of species (Fig. 1*A*). Moreover, greater than 60% of trait variation is bounded along one functional plane based on species ordination using Principal Correspondence Analysis (PCoA) (Fig. 1*A*).

The first axis of variation (which explains 35.92%) identifies one extreme, typified by species that are typically sessile and large, have symbiotic relationships with chemosynthetic bacteria and contribute complexity to the habitat (Fig. 1*B*). This set of traits corresponds to iconic foundation species dominating biomass at vent communities (4, 30) (e.g., the giant tube worm *R. pachyptila* and the mussel *Gigantidas tangaroa*) (Fig. 1*A*). At the other extreme, species are freely mobile, small, heterotrophic and do not add complexity to the habitat (Fig. 1*B*), representing the abundant species exploiting vent primary productivity (e.g., the amphipod *Bouvierella curtirama* and the scale worm *Harmothoe globosa*) (Fig. 1*A*). Along the second axis of variation (which explains 26.57%), species distribute along a functional

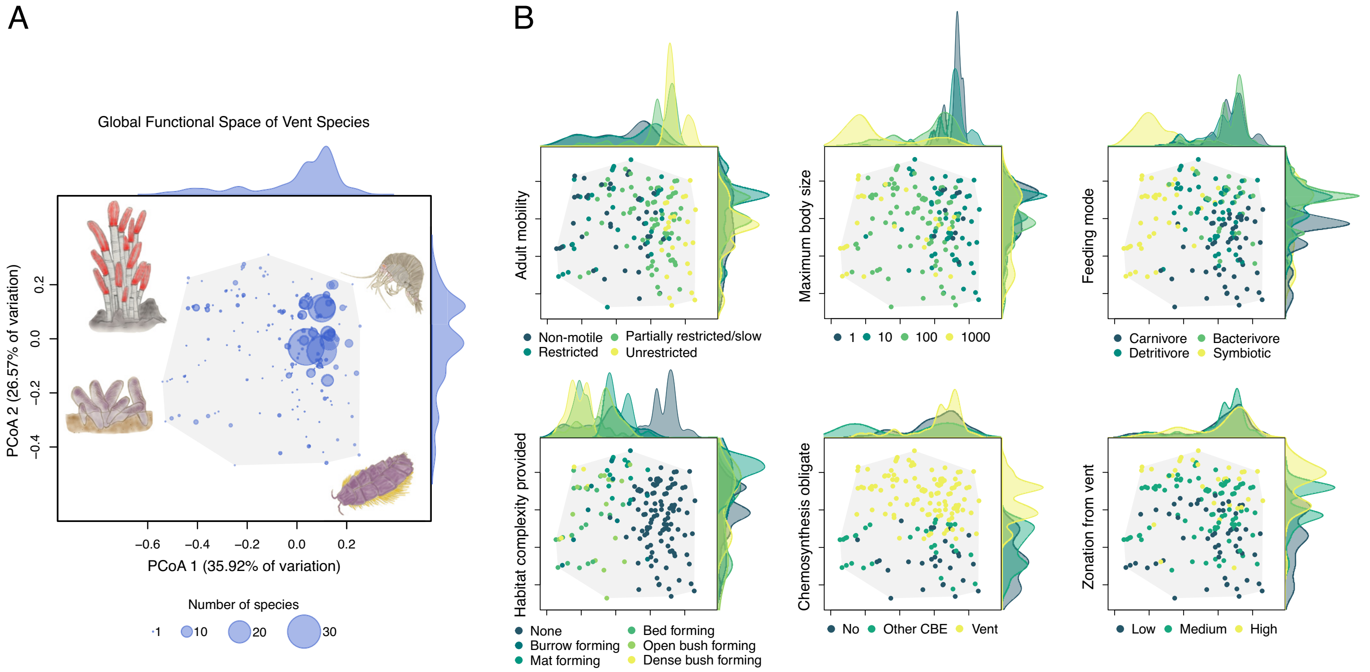

Fig. 1. The global functional space of vent species and their functional strategies. (*A*) Global pool of unique trait combinations (n= 167) distributed along the first two PCoA axes synthesizing 62.5% of trait variation. Unique trait combinations are weighted by the number of species. The species distribution density is shown along axes on the top and right side. Drawings highlight "archetype" species representing ends of the continuum of ecological strategies uncovered, that is, from the giant tubeworm *Riftia pachyptila* and the mussel *Gigantidas tangaroa* (*Left*) to the amphipod *Bouvierella curtirama* and the scale worm *Harmothoe globosa* (*Right*), and from *G. tangaroa* and *H. globosa* (*Bottom*) to *R. pachyptila* and *B. curtirama* (*Top*) (*B*) Distribution of categories for each trait along the global functional space. Trait distribution densities along axes are shown on the top and right side of the PCoA.

continuum of habitat specialization. At one extreme of this axis, species belong exclusively to vent habitats (Chemosynthesis obligate: “Vent”) and inhabit microhabitats under higher environmental stress, i.e., high and diffuse-fluid-flux areas (Zonation from vent: “High” and “Medium”, e.g., *R. pachyptila* and *B. curtirama*) (Fig. 1*B*). At the other extreme, species also occur in other chemosynthetic (Chemosynthesis obligate: “Other CBE”) or non-chemosynthetic deep-sea environments (Chemosynthesis obligate: “No”) and inhabit less stressful microhabitats, i.e., diffuse fluid-flux and periphery areas (Zonation from vent: “Medium” and “Low”, e.g., *G. tangaroa* and *H. globosa*) (Fig. 1*B*). These continuums along two functional axes imply that certain trait combinations are rare or nonexistent explaining the low number of realized unique trait combinations. For instance, foundation species were not highly mobile, and vice versa (Fig. 1*B*). Similarly, species shared with other chemosynthetic and non-chemosynthetic deep-sea habitats rarely inhabit high-fluid flux microhabitats (Fig. 1*B*) highlighting that vent endemics require specific adaptations to harsh environmental regimes presented by venting fluid and hard substrata (31, 32).

Some species pools show a distinct functional trait composition. We assessed regional functional turnover, the non-overlapping functional space, through pairwise comparison and verified null expectations assuming a random species distribution (*Materials and Methods*). In ca. 30% of the pairwise regional comparisons, turnover is greater than expected based on null models (SES > 1.96); however, these mainly involve species from the Mohns Ridge and/or the East Pacific suggesting that only these two regions host functionally distinct species pools (Fig. 2*A*). We also find that these two regions show opposed patterns of functional dispersion as revealed by null expectations under random species distribution. Specifically, the East Pacific region, as well as the Indian Ridge, display lower functional dispersion (SES < −1.96) suggesting that their species pools have low functional diversity (Fig. 2*B*). By contrast, the Mohns Ridge and Guaymas Basin species pools show higher functional dispersion than expected (SES > 1.96) indicating that they contain taxa with very distinct traits and thus constitute functional hotspots (Fig. 2*B*). Null models also reveal that redundancy is higher than expected (SES > 1.96) in more than 50% of the regions including the East Pacific, East Scotia Ridge, Kermadec Arc, Mid-Atlantic Ridge, Okinawa Trough, and South West Pacific (Fig. 2*B*) supporting the hypothesis that vent environments select for species with similar ecological strategies in these regions.

Despite the fundamental similarities in the geochemical nature of the fluids that sustain these chemosynthetic communities, we find notable differences in the functional traits among regions. For instance, the evolution of biogeographical connections (e.g., 31, 33–35) is one likely driver of differences in the case of Mohns Ridge communities. The vents here lack vent endemics including chemosymbiotic foundation species (Fig. 3 and *SI Appendix*, Fig. S2) due to geological and hydrographic barriers to exchange with Pacific and Mid-Atlantic Ridge fauna (28, 33). The proximity to continental shelves and seeps enabled colonization of Mohns Ridge vents by fauna from other reducing environments, such as sunken wood and seeps (36, 37), and Arctic-tolerant background species, including uncommon vent inhabitants such as sponges (33). The resulting unique, nonendemic communities composed of fauna with very particular traits rarely seen in other hydrothermal vents thus drive the distinct functional composition of Mohns Ridge and its high functional dispersion.

Tectonic dynamics also may shape functional trait distribution. Despite the East Pacific being the most species-rich region, it is missing foundation vent species that occur at other chemosynthesis-based habitats, such as seeps and organic falls, and that inhabit lower fluid-flow microhabitats and/or periphery (Fig. 3 and *SI Appendix*, Fig. S2). Indeed, East Pacific vents are distant from seeps and are hosted on bare basalt with few, if any, sedimented reducing niches for the establishment of seep species or species from other deep-sea habitats (31). Furthermore, some East Pacific Rise sections suffer frequent catastrophic volcanic eruptions that wipe out entire communities, precluding succession to ecological climax (38–41). The frequent disturbances and reduced habitat availability could constrain the functional space occupied by the East Pacific species pool and drive its distinct functional composition, low dispersion, and redundancy.

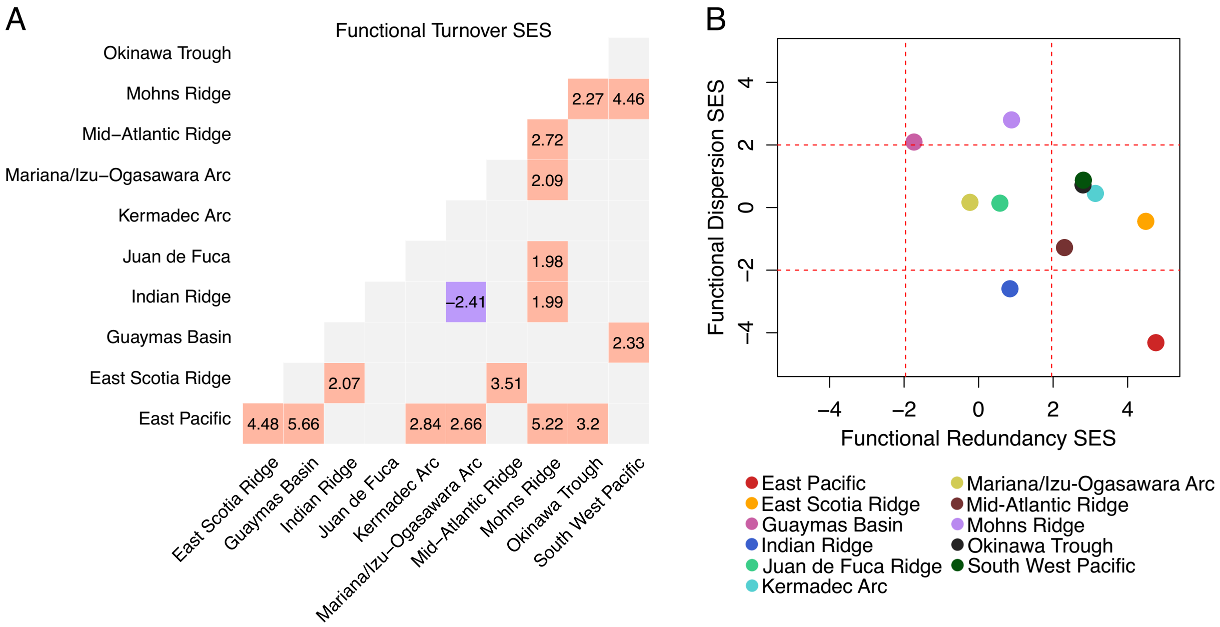

Fig. 2. Standard effect sizes (SES) of functional metrics at the regional scale. (*A*) Pairwise comparisons of the functional space not shared between regions (functional turnover). Red, blue, and gray cells indicate SES values higher, lower, and as expected by chance, respectively, based on null models of random species distributions between the compared regions. (*B*) Functional dispersion and redundancy. Values over 1.96 or lower than −1.96 (red dashed lines) are considered values higher and lower than expected by chance based on null models of random species distributions across regions.

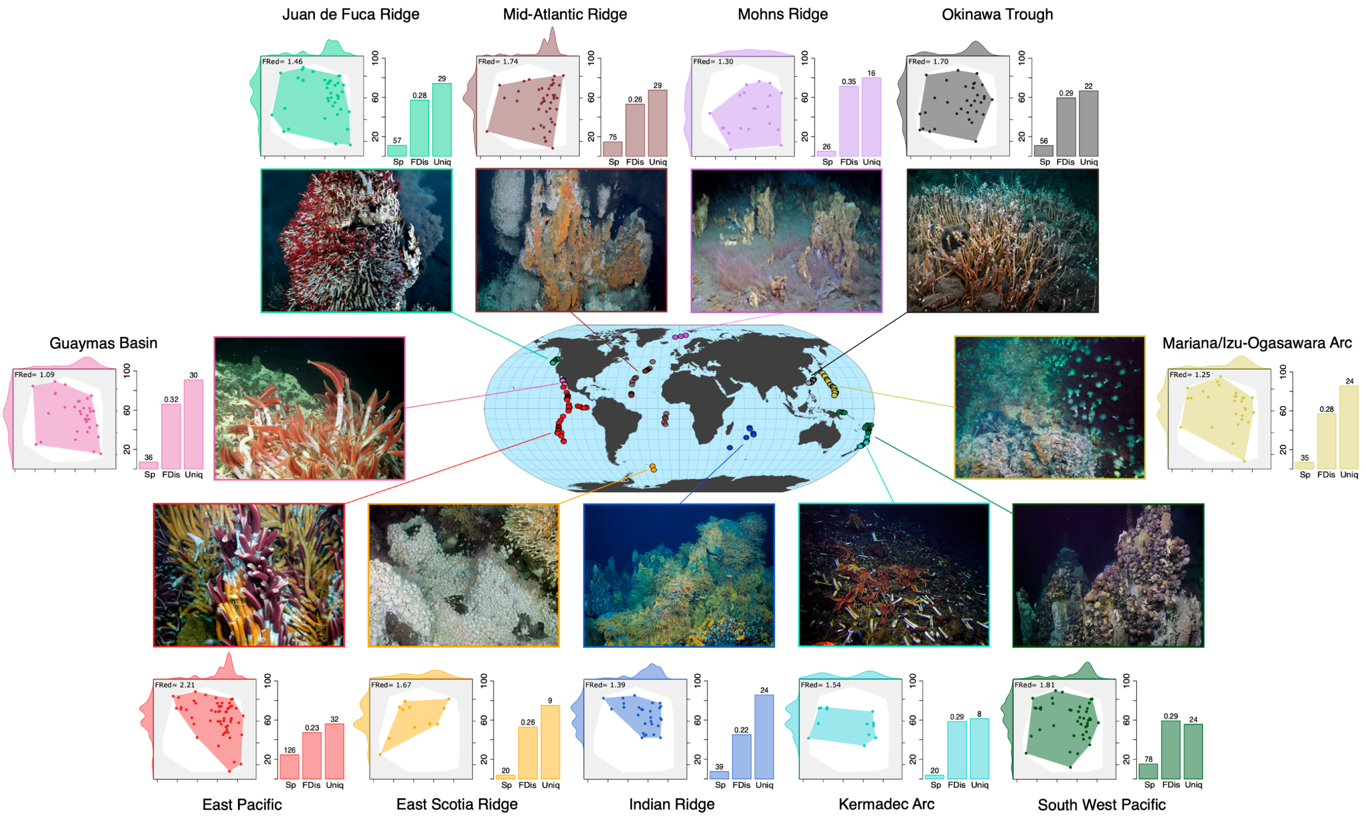

Fig. 3. Global distribution of vent regions and their functional patterns. Functional space of regions (colored polygons) and pools of species (dots) along the first two PCoA axes are shown within the global functional space (white polygon). Species with identical trait combinations are superimposed. Species distribution density along axes are shown on the top and right sides. Bars show the percentage of species (Sp), functional dispersion (FDis), and unique trait combinations represented by one species (Uniq). Sp and FDis are expressed as percentages of the global totals whereas Uniq is expressed as percentage of each regional pool (raw values showed on the bar tops). The functional redundancy (FRed) is indicated for each functional space. Image credits: Juan de Fuca (Ocean Networks Canada), Mid-Atlantic Ridge and East Pacific (Ifremer), Mohns Ridge (University of Bergen), Okinawa Trough (Chong Chen/JAMSTEC), Mariana/Ogasawara Arc (NOAA/WHOI), South West Pacific and Guaymas Basin (Schmidt Ocean Institute); Kermadec Arc (NOAA/NIWA), Indian Ridge (Jon Copley/University of Southampton), and East Scotia Ridge (27).

Environmental variability may also influence the functional composition and distinctions among regional species pools. The functional turnover between the East Pacific and Guaymas Basin regions is higher than expected based on our null expectations (Fig. 2*A*). Guaymas Basin vents are evolutionarily related to the East Pacific vents and share eight species in our database including the giant tubeworm *R. pachyptila* (34). By comparison, vents at Guaymas Basin are hosted in a more stable, sedimentary basin with reducing sediments and share species with the nearby continental margins and cold seeps (32, 42). Indeed, Guaymas Basin vents may play a pivotal role in the transition and radiation of faunal lineages between sedimented cold seeps and hot, bare-rock vents in the Pacific (31). The heterogeneity of habitats in Guaymas Basin compared to those in the East Pacific thus likely drives observed differences in functional composition, despite evolutionary relationship between these regions, and promotes high functional dispersion of Guaymas fauna.

The percentage of unique trait combinations represented by a single species (Uniq) is more than 50% of the total combinations in each regional species pool (Fig. 3). Specifically, unique trait combinations represented by one species range from 56% of the total unique trait combinations in the East Pacific to 91% in Guaymas Basin (see “Uniq” bars: Fig. 3). These values agree with null expectations under random species distribution in over 70% of regional species pools indicating that a high number of unique trait combinations represented by a single species is a common characteristic of the world’s vent regions (*SI Appendix*, Fig. S3). Given the low richness of vent systems, unique trait combinations will typically be represented by a single species versus multiple redundant species. Indeed, we observe that half of the total 197 unique trait combinations in our global species dataset are represented by a single species (*SI Appendix*, Fig. S4). Moreover, unique trait combinations represented by one species are evenly distributed across the global functional space and are also dispersed across taxonomic groups. Thus, particular traits and taxa are not associated with functional uniqueness (*SI Appendix*, Fig. S4).

The selection of traits, how the different categories within each trait are assessed, and sampling bias can lead to most unique trait combinations being represented by only a single species (19). However, the patterns uncovered in our analysis are not likely due to the trait scoring methods we selected or to sampling bias. First, we performed sensitivity tests, rerunning analyses after removing one trait at a time and collapsing trait categories to fewer categories (*Materials and Methods*). These tests show that unique trait combinations represented by one species are almost never lower than the 50% of the total combinations at any given regional species pool; our results therefore appear robust to potential methodological bias related to trait and category selection (*SI Appendix*, Tables S1–S6 and Fig. S5). Second, our findings do not result from sampling bias because even in the most heavily sampled regions, such as the East Pacific (126 species) and the Mid-Atlantic Ridge (75 species), functionally unique species are the majority (~56% and ~67% of the regional species pool) (Fig. 3). Thus, the many functionally unique species that we find are likely an outcome of low species richness in a system where the species pool is small at all scales with unfilled functional space.

Our findings further highlight that extinction could lead to a quick loss of function. We simulated species extinctions assuming equal probability of extinctions and no dependencies between species. To remove 50% of the functional space (functional richness) required species removals ranging from 29% (Kermadec Arc) to 57% (Southwest Pacific) (Fig. 4). In highlighting the potential reduction of overall functional space with species loss, we note that both rare and common species make unique contributions to functional diversity at vents (9). Thus, we find poor insurance against functional loss because the extinction of one species, on average, represents loss of a species with a unique ecological role.

Although species extinctions are influenced by traits related to the causes of extinction (23, 43) and are not random, current data are insufficient to assign trait-based probabilities of extinction. However, the dominant model of connectivity in deep-sea hydrothermal vents is the stepping stone model (e.g., refs. 44 and 45). This model implies that the removal of a local population could eventually starve a highly dispersive species of recruits. Moreover, most vent species have restricted distribution ranges, and they are often known only from one to a few vent sites, e.g., Northwest and Southwest Pacific regions (46–48), Juan de Fuca Ridge (46), the Mid-Atlantic Ridge (49). Wholesale removal of vent sites by mining, trawling, or other impacts will likely take out species from the regional species pool that have a restricted distribution. The disruption of the metapopulation by removing a site may therefore have catastrophic effects. Thus, we suggest that, in view of lack of better data and the presence of constraining factors, a "random removal" of species is a reasonable approximation.

Vent communities will likely be heavily altered if invaded by exotic species and pathogens; a common impact of human expansion (50, 51). Any regional gains in species will likely come with functional consequences as invasive species often differ functionally from resident native species (52). Many vent species are unique, based on their trait combinations, and functional spaces show unfilled gaps in all regions suggesting that invasive species can exploit gaps in ecological niches or functional space left by native species (53). When such gaps occur, invasive species may find favorable conditions to establish and thrive, sometimes outcompeting native species for resources and altering entire community species composition and functioning (52, 53). As human activities increase in the deep ocean, the potential transmission of species and pathogens to vent systems is a concern (54, 55).

This first look at the global picture of vent functional diversity has important implications for vent responses to disturbances and human impacts. Hydrothermal vent ecosystems are listed by the United Nation's FAO as a "Vulnerable Marine Ecosystem" because the available habitat is typically only meters in size and many species are endemic (25). Ocean changes and anthropogenic threats will likely have strong impacts for many vent species as human activities and their influence increase in the deep sea (7, 56, 57). Deoxygenation and changing currents may influence species larvae, while destructive activities such as mining will reduce habitat availability and habitat quality impacting both species with large and restricted geographic ranges or those with small source population areas (25, 56).

Successful restoration is unlikely in these extreme, unusual, and remote environments (25) where endemic species will be highly vulnerable to extinction (58). Moreover, the loss of species can erode functional diversity (23, 43) and ecosystem functioning, as the numbers and types of species representing unique morphological, physiological, and/or behavioral characteristics (59, 60) relate to contributions to ecosystem functions and services (61–63). Even though seafloor vent habitats cover only ~50 km^2 worldwide (25), vents play important roles in global ocean micronutrients and carbon cycling (64, 65) affecting both shallow and deep systems (4, 65), are areas of endemic genetic resources for the development of new biotechnology and pharmaceutical products, and act as invaluable technological, educational, and inspirational sources [reviewed in (25)].

Our findings indicate that the small pools of vent species have many functionally unique species. Species losses, as simulated here, will likely lead to functional loss as observed in more accessible habitats (43), with the potential for negative societal consequences (61). Moreover, many vent regions appear to have many empty niches available and could be vulnerable to species introductions (54, 55). Given the ubiquitous high rates of species extinctions and invasions in accessible habitats, this high functional vulnerability

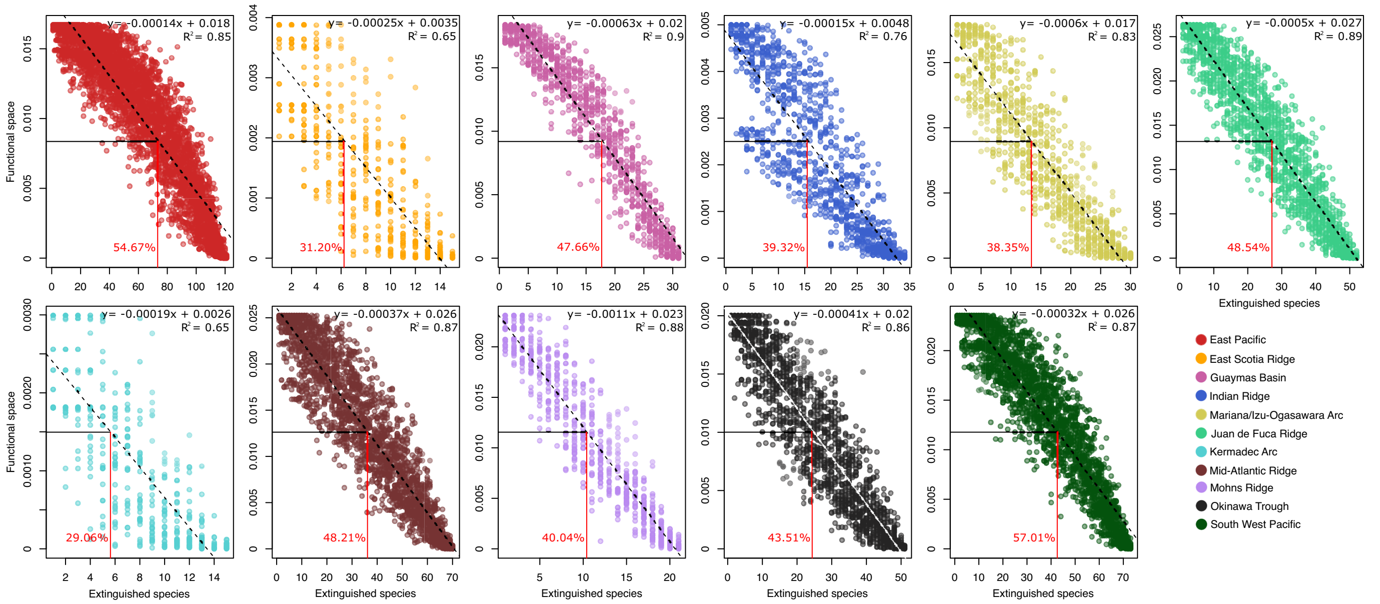

Fig. 4. Simulated extinction of species and its effect on the extent of function (functional richness) of vent regions. For comparison, the proportion of extinguished species (vertical solid red line) needed to reduce the functional range (functional richness) to half (horizontal solid black line) is indicated for each region. Model parameters, $R^{2,}$ and regression lines (dashed lines) are shown for each region.

calls for aggressive protection measures on vent habitats, one of the last great wildernesses on Earth (25, 56).

Materials and Methods

Species and Trait Data Selection and Processing. We assembled and adapted taxonomic and trait data from the sFDvent database (26), a global effort to compile species and their biological traits for deep-sea hydrothermal vent fauna. The taxonomic data in sFDvent are biased by sampling intensity, as some regions have been visited and studied for more years than others. Thus, to address potential sources of bias, we excluded Foraminifera species, vagrant species that only enter vent habitats occasionally (63 species), and species belonging to groups usually considered meiofauna (i.e., copepod, nematode, mite, and ostracod species–84 species). Sampling of these groups has been mostly limited to few vents and would artificially inflate uniqueness due to undersampling or underidentification. We also added 28 species originally not included in the sFDvent database but reported in Desbruyères et al. 2006. The final dataset consisted of 511 taxa. Here, we will refer to these taxa as "species", as we only included species yet to be formally named if they: i) could be linked to a taxonomist soon to identify them, and/or ii) were known to be distinct from other species in the sFDvent database, according to expert knowledge.

We selected six ordinal/categorical traits from sFDvent to characterize the functional strategies of vent species. The scoring of these traits was designed for fauna for which relatively few specimens are available and for which sampling is relatively difficult and expensive (26). Ordered traits were scored according to specialism or adaptation required. Relative Adult Mobility was coded using four ordered categories: nonmotile, restricted movement, partially restricted movement and/or slow, and unrestricted movement. Estimated Maximum Body Size was coded using four ordered categories representing size on a log scale: ≤1 mm, 1.1 to 10 mm, 10.1 to 100 mm, and ≥100.1 mm. Chemosynthesis Obligate was coded using three ordered categories: species not exclusively found at chemosynthetic ecosystems, other CBE (species found at vents and other chemosynthesis-based ecosystems), and vent (species exclusively found at vent habitats). Zonation from Vent was coded using three ordered categories: periphery (species inhabiting vent periphery), medium (species inhabiting diffuse flow areas), and high (species inhabiting focused flow areas). Habitat Complexity Provided was coded using six categories: none, burrow forming, mat forming, bed forming, open bush forming, and dense bush forming. We merged three traits from sFDvent (Position of Symbiont, Nutritional Source and Trophic Mode) to derive a trait, Feeding Mode, coded as four categories: symbiotic, bacterivore, detritivore, and carnivore. We achieved full trait coverage for all species and traits by completing the sFDvent information with data from published literature and authors' expertise. Our data are provided at https://github.com/DeepEcology/Functional_Diversity_DeepSea_Vents (66).

Hydrothermal Vent Region Delineation. We analyzed the global biogeography of deep-sea hydrothermal vents to identify coherent regions with homogeneous species pools. We included recently sampled regions such as the East Scotia Ridge in Antarctica (27), the central and SW Indian Ocean regions (29), and the Arctic Mohns Ridge (28, 33) which were not simultaneously considered in previous global analyses (1, 27, 35, 67). Species in the sFDvent database were assigned location information by expert contributors, but this information could not be used in the format provided, as locations varied in spatial resolution and scale. Thus, we assigned each location to a region, as indicated in the InterRidge vent database [v.3.4 (68)]. We ran a hierarchical clustering analysis using the Sørensen's distance on taxonomic (presence–absence) data with the average-linkage approach using the hclust function in the stats R package (69). The same cluster analysis was repeated using the Ward's linkage approach to avoid potential bias related to the linkage method (*SI Appendix*, Fig. S6). We then visually identified the number of coherent taxonomic clusters that i) separated at a relatively higher confidence and ii) did not overseparate clusters, inflating dissimilarity.

Global Functional Space of Vent Fauna. We estimated pairwise functional distances between all vent species using the Gower distance, weighting traits equally to ensure their equal contribution and treating ordered traits as ranks (method "metric"), using the func.dist function of the mFD R package (70). From there, we computed a Principal Coordinates Analysis (PCoA) to distribute species in a multidimensional space based on their functional dissimilarities and create a "global functional space" of vent species using the quality.fspaces function of the mFD R package (70).

Functional Convergence of Vent Regional Species Pools. To test whether regional species pools converge functionally, we assessed the turnover component of the functional ß-diversity between pairs of regions, i.e., the portion of the functional space not shared between the compared regions (71, 72). We calculated the functional space of regions by estimating their convex hull volumes within the global functional space, that is, the functional volumes in the global multidimensional functional space encapsulating all species of each region. We kept the first four principal axes, which produced the highest-quality multidimensional space as identified by the Mean Absolute Deviation (MAD) index using the quality.fspaces function of the mFD R package (70, 73). We then estimated the functional turnover between pairs of regions using the Jaccard dissimilarity index computed with the functional.beta.pair function of the betapart R package (74). Jaccard functional turnover increases, i.e., indicates more dissimilarity, when there is no overlap between regional functional spaces and decreases with increasing functional overlap between regions, independently of regional functional volume difference (72). The functional turnover observed could be driven only by the species richness differences between vent regions (71, 72). Thus, to test the significance of functional turnover while accounting for the species richness differences, we created null models that shuffled species between the compared regions, while maintaining observed regional species richness and species occurrence frequency, and compared the observed values to those of null expectations. This process was repeated 1,000 times in each comparison and the observed (F_{obs}) and null (F_{null}) values were compared using the standardized effect size (SES) (75):

$$\mathrm{SES} = \left[F_{obs} - \mathrm{mean}\left(F_{null}\right)\right] / \mathrm{SD}\left(F_{null}\right),$$

SES functional values were considered higher or lower than expected at random if greater or lower than 1.96 and -1.96, respectively. Randomizations were performed using the independent swap algorithm of the function *RandomizeMatrix* in the R package picante (76).

Functional Dispersion, Redundancy, and Functionally Unique Species of Vent Regions. To test whether vent environment selects for species with similar traits, we computed the functional redundancy, FRed, as mean number of species per unique trait combination for each region (19). We also computed the functional dispersion, FDis, as the average distance of species from the functional center of gravity (77), to identify regions that show higher or lower trait dissimilarity in their species pool. Finally, we assessed the abundance of functionally unique species per region by estimating the percentage of unique trait combinations represented by only one species (Uniq), which has been called the functional vulnerability index elsewhere (19). FDis was computed and scaled using the alpha.fd.multidim function, and FRed and Uniq were computed using the alpha.fd.fe both of the mFD R package (70). To test the significance of these indices while accounting for the potential influence of species richness across vent regions, we compared the observed values to those of null expectations using a null model. The null model randomly shuffled species across all regions while maintaining observed regional species richness and species occurrence frequency in the global pool. This process was repeated 1,000 times and observations were compared using the standardized effect size (SES) as described above.

Sensitivity Analyses. We assessed whether our results were influenced by the categories of each trait and/or the selection of which traits were included (19). First, we rescored some traits to include fewer categories to constrain the number of potential unique trait combinations. Specifically, the Chemosynthesis Obligate trait was rescored in two categories: species exclusively occurring at chemosynthesis-based ecosystems ("vent" and "other CBE" categories in the original classification) and species also occurring at nonchemosynthesis deep-sea habitats. The Habitat Complexity Provided trait was rescored in two categories: species adding complexity ("bed forming", "burrow forming", "dense bush forming", "mat forming", and "open bush forming" species in the original classification) and species not adding complexity. Zonation from Vent was rescored in two categories: species occurring at areas directly influenced by hydrothermal fluids ("high" and "medium" in the original classification) and species occurring at peripheries. Second, we reran analyses deleting one trait each time to identify whether our results were overly influenced by a single trait.

Data, Materials, and Software Availability. R scripts and analyzed dataset data have been deposited in https://github.com (https://github.com/DeepEcology/Functional_Diversity_DeepSea_Vents) (66).

ACKNOWLEDGMENTS. J.M.A.-L. salary was through institutional funds from the University of Victoria awarded as part of A.E.B.'s Impact Chair position. A.S.A.C. acknowledges funding from the SPITFIRE Doctoral Training Partnership (supported by the Natural Environmental Research Council, grant number: NE/L002531/1) and the University of Southampton, as well as time supported by the Sustainable and Healthy Food Systems programme, supported by the Wellcome Trust's Our Planet, Our Health programme (Grant number: 205200/Z/16/Z). The Wellcome Trust had no role in the design, analysis, or writing of this article. A.S.A.C. also acknowledges the support of Carole Dalin and Sam Southgate. V.T. acknowledges the support from the Natural Sciences and Engineering Research Council of Canada. sFDvent (which comprised the core dataset for this paper) was designed following working group support by sDiv, the Synthesis Centre of iDiv (DFG FZT 118). Two anonymous reviewers made helpful recommendations to an earlier version of this manuscript.

1. C. L. Van Dover, C. German, K. Speer, L. Parson, R. Vrijenhoek, Evolution and biogeography of deep-sea vent and seep invertebrates. *Science* **295**, 1253–1257 (2002).
2. G. W. Luther III *et al.*, Chemical speciation drives hydrothermal vent ecology. *Nature* **410**, 813 (2001).
3. A. E. Bates, R. W. Lee, V. Tunnicliffe, M. D. Lamare, Deep-sea hydrothermal vent animals seek cool fluids in a highly variable thermal environment. *Nat. Commun.* **1**, ncomms1014 (2010).
4. N. Le Bris *et al.*, Hydrothermal energy transfer and organic carbon production at the deep seafloor. *Front. Marine Sci.* **5**, 531 (2019).
5. L. S. Mullineaux *et al.*, Exploring the ecology of deep-sea hydrothermal vents in a metacommunity framework. *Front. Marine Sci.* **5**, 49 (2018).
6. S. Mitarai, H. Watanabe, Y. Nakajima, A. F. Shchepetkin, J. C. McWilliams, Quantifying dispersal from hydrothermal vent fields in the western Pacific Ocean. *Proc. Natl. Acad. Sci. U.S.A.* **113**, 2976–2981 (2016).
7. E. Ramirez-Llodra *et al.*, Man and the last great wilderness: Human impact on the deep sea. *Plos One* **6**, e22588 (2011).
8. C. L. Van Dover, Impacts of anthropogenic disturbances at deep-sea hydrothermal vent ecosystems: A review. *Mar. Environ. Res.* **102**, 59–72 (2014).
9. A. S. Chapman, V. Tunnicliffe, A. E. Bates, Both rare and common species make unique contributions to functional diversity in an ecosystem unaffected by human activities. *Divers. Distrib.* **24**, 568–578 (2018).
10. J. S. Joswig *et al.*, Climatic and soil factors explain the two-dimensional spectrum of global plant trait variation. *Nat. Ecol. Evol.* **6**, 36–50 (2022).
11. D. S. Maynard *et al.*, Global relationships in tree functional traits. *Nat. Commun.* **13**, 3185 (2022).
12. D. J. G. Inward, R. G. Davies, C. Pergande, A. J. Denham, A. P. Vogler, Local and regional ecological morphology of dung beetle assemblages across four biogeographic regions. *J. Biogeogr.* **38**, 1668–1682 (2011).
13. D. L. Mahler, T. Ingram, L. J. Revell, J. B. Losos, Exceptional Convergence on the Macroevolutionary Landscape in Island Lizard Radiations. *Science* **341**, 292–295 (2013).
14. B. G. Holt *et al.*, Environmental variation is a major predictor of global trait turnover in mammals. *J. Biogeogr.* **45**, 225–237 (2018).
15. I. Conenna *et al.*, Global patterns of functional trait variation along aridity gradients in bats. *Glob. Ecol. Biogeogr.* **30**, 1014–1029 (2021).
16. A. M. Lawing, J. T. Eronen, J. L. Blois, C. H. Graham, P. D. Polly, Community functional trait composition at the continental scale: The effects of non-ecological processes. *Ecography* **40**, 651–663 (2017).
17. C. Ibañez *et al.*, Convergence of temperate and tropical stream fish assemblages. *Ecography* **32**, 658–670 (2009).
18. M. McLean *et al.*, Trait similarity in reef fish faunas across the world's oceans. *Proc National Acad. Sci.* **118**, e2012318118 (2021).
19. D. Mouillot *et al.*, Functional over-redundancy and high functional vulnerability in global fish faunas on tropical reefs. *Proc. Natl. Acad. Sci. U.S.A.* **111**, 13757–13762 (2014).
20. K. M. Scott, C. R. Fisher, Physiological ecology of sulfide metabolism in hydrothermal vent and cold seep vesicomyid clams and vestimentiferan tube worms. *Am. Zool.* **35**, 102–111 (1995).
21. M. L. Jones, *Riftia pachyptila*, new genus, new species, the vestimentiferan worm from the Galápagos Rift geothermal vents (Pogonophora). *Proc. Biol. Soc. Washington* **93**, 1295–1313 (1980).
22. E. Beccari, P. Capdevila-Lanzaco, R. Salguero-Gomez, C. P. Carmona, Mammal life history strategies are strongly associated with environmental realms Summary. bioXriv [Preprint] (2023), https://doi.org/10.1101/2023.06.29.546851 (Accessed 8 December 2023).
23. R. S. C. Cooke, F. Eigenbrod, A. E. Bates, Projected losses of global mammal and bird ecological strategies. *Nat. Commun.* **10**, 2279 (2019).
24. S. Díaz *et al.*, The global spectrum of plant form and function. *Nature* **529**, 167–171 (2016).
25. C. L. Van Dover *et al.*, Scientific rationale and international obligations for protection of active hydrothermal vent ecosystems from deep-sea mining. *Marine Policy* **90**, 20–28 (2018).
26. A. S. Chapman *et al.*, sFDvent: A global trait database for deep-sea hydrothermal-vent fauna. *Glob. Ecol. Biogeogr.* **28**, 1538–1551 (2019). https://doi.org/10.1111/geb.12975.
27. A. D. Rogers *et al.*, The Discovery of New Deep-Sea Hydrothermal Vent Communities in the Southern Ocean and Implications for Biogeography. *Plos Biol.* **10**, e1001234 (2012).
28. R. B. Pedersen *et al.*, Discovery of a black smoker vent field and vent fauna at the Arctic Mid-Ocean Ridge. *Nat. Commun.* **1**, 126 (2010).
29. J. T. Copley *et al.*, Ecology and biogeography of megafauna and macrofauna at the first known deep-sea hydrothermal vents on the ultraslow-spreading Southwest Indian Ridge. *Sci. Rep.* **6**, 39158 (2016).
30. B. Govenar, "Shaping vent and seep communities: Habitat provision and modification by foundation species" in *The Vent and Seep Biota Aspects from Microbes to Ecosystems*, S. Kiel, Ed. (Springer, 2010), pp. 403–432.
31. S. Kiel, A biogeographic network reveals evolutionary links between deep-sea hydrothermal vent and methane seep faunas. *Proc. R. Soc. B* **283**, 20162337 (2016).
32. M. Portail *et al.*, Comparative study of vent and seep macrofaunal communities in the Guaymas Basin. *Biogeosciences* **12**, 5455–5479 (2015).
33. C. Schander *et al.*, The fauna of hydrothermal vents on the Mohn Ridge (North Atlantic). *Mar. Biol. Res.* **6**, 155–171 (2010).
34. V. Tunnicliffe, C. M. R. Fowler, Influence of sea-floor spreading on the global hydrothermal vent fauna. *Nature* **379**, 531–533 (1996).
35. Y. Moalic *et al.*, Biogeography revisited with network theory: Retracing the history of hydrothermal vent communities. *Systematic Biol.* **61**, 127–137 (2012).
36. M. N. Georgieva *et al.*, A chemosynthetic weed: The tubeworm Sclerolinum contortum is a bipolar, cosmopolitan species. *BMC Evol. Biol.* **15**, 1–17 (2015).
37. M. H. Eilertsen *et al.*, Genetic connectivity from the arctic to the antarctic: Sclerolinum contortum and Nicomache lokii (Annelida) are both widespread in reducing environments. *Sci. Rep.* **8**, 4810 (2018).
38. R. M. Haymon *et al.*, Volcanic eruption of the mid-ocean ridge along the East Pacific Rise crest at 9°45–52′N: Direct submersible observations of seafloor phenomena associated with an eruption event in April, 1991. *Earth Planet. Sci. Lett.* **119**, 85–101 (1993).
39. T. M. Shank *et al.*, Temporal and spatial patterns of biological community development at nascent deep-sea hydrothermal vents (9°50′N, East Pacific Rise). *Deep Sea Res. Part II Top Stud. Oceanogr.* **45**, 465–515 (1998).
40. L. N. Dykman, S. E. Beaulieu, S. W. Mills, A. R. Solow, L. S. Mullineaux, Functional traits provide new insight into recovery and succession at deep-sea hydrothermal vents. *Ecology* **102**, e03418 (2021).
41. L. S. Mullineaux *et al.*, Prolonged recovery time after eruptive disturbance of a deep-sea hydrothermal vent community. *Proc. Royal. Soc. B* **287**, 20202070 (2020).
42. M. Portail *et al.*, Food-web complexity in Guaymas Basin hydrothermal vents and cold seeps. *Plos One* **11**, e0162263 (2016).
43. C. P. Carmona *et al.*, Erosion of global functional diversity across the tree of life. *Sci. Adv.* **7**, eabf2675 (2021).
44. R. C. Vrijenhoek, Genetic diversity and connectivity of deep-sea hydrothermal vent metapopulations. *Mol. Ecol.* **19**, 4391–4411 (2010).
45. C. Breusing *et al.*, Biophysical and population genetic models predict the presence of ‘"phantom"’ stepping stones connecting mid-atlantic ridge vent ecosystems. *Curr. Biol.* **26**, 1–11 (2016).
46. T. N. Giguère, V. Tunnicliffe, Beta diversity differs among hydrothermal vent systems: Implications for conservation. *PLoS ONE* **16**, e0256637 (2021).
47. O. Brunner *et al.*, Species assemblage networks identify regional connectivity pathways among hydrothermal vents in the Northwest Pacific. *Divers Distrib.* **12**, e9612 (2022).
48. V. Tunnicliffe *et al.*, Hydrothermal vent fauna of the western Pacific Ocean: Distribution patterns and biogeographic networks. *Divers Distrib.* **30**, e13794 (2023).
49. R. Boschen-Rose, A. Colaco, Northern mid-atlantic ridge hydrothermal habitats: A systematic review of knowledge status for environmental management. *Front. Mar. Sci.* **8**, 657358. (2021).
50. D. A. Burney, T. F. Flannery, Fifty millennia of catastrophic extinctions after human contact. *Trends Ecol. Evol.* **20**, 395–401 (2005).
51. H. A. Mooney, E. E. Cleland, The evolutionary impact of invasive species. *PNAS* **98**, 5446–5451 (2010).
52. B. Gallardo *et al.*, Global ecological impacts of invasive species in aquatic ecosystems. *Glob. Change Biol.* **22**, 151–163 (2016).
53. L. Gallien, M. Carboni, The community ecology of invasive species: Where are we and what's next? *Ecography* **40**, 335–352 (2017).
54. C. L. Van Dover *et al.*, A fungal epizootic in mussels at a deep-sea hydrothermal vent. *Mar. Ecol.* **28**, 54–62 (2007).
55. J. R. Voight *et al.*, Scientific gear as a vector for non-native species at deep-sea hydrothermal vents. *Conserv. Biol.* **26**, 938–942 (2012).
56. H. J. Niner *et al.*, Deep-sea mining with no net loss of biodiversity–An impossible aim. *Front. Mar. Sci.* **5**, 53 (2018).
57. L. A. Levin, N. Bris, The deep ocean under climate change. *Science* **350**, 766–768 (2015).
58. J. D. Sigwart *et al.*, Red Listing can protect deep-sea biodiversity. *Nat. Ecol. Evol.* **3**, 1134–1134 (2019).
59. S. Díaz, M. Cabido, Vive la différence: Plant functional diversity matters to ecosystem processes. *Trends Ecol. Evol.* **16**, 646–655 (2001).
60. C. Violle *et al.*, Let the concept of trait be functional!. *Oikos* **116**, 882–892 (2007).
61. B. J. Cardinale *et al.*, Biodiversity loss and its impact on humanity. *Nature* **486**, 59–67 (2012).
62. D. U. Hooper *et al.*, Effects of biodiversity on ecosystem functioning: A consensus of current knowledge. *Ecol. Monogr.* **75**, 3–35 (2005).
63. T. H. Oliver *et al.*, Biodiversity and resilience of ecosystem functions. *Trends Ecol. Evol.* **30**, 673–684 (2015).
64. J. A. Resing *et al.*, Basin-scale transport of hydrothermal dissolved metals across the South Pacific Ocean. *Nature* **523**, 200 (2015).
65. M. Ardyna *et al.*, Hydrothermal vents trigger massive phytoplankton blooms in the Southern Ocean. *Nat. Commun.* **10**, 2451 (2019).

66. J. M. Alfaro-Lucas, Data from "Functional Diversity of World's Deep-Sea Vents". GitHub. https://github.com/DeepEcology/Functional_Diversity_DeepSea_Vents. Deposited 6 December 2023.
67. C. Bachraty, P. Legendre, D. Desbruyères, Biogeographic relationships among deep-sea hydrothermal vent faunas at global scale. *Deep Sea Res. Part Oceanogr. Res. Pap.* **56**, 1371–1378 (2009).
68. S. E. Beaulieu, K. M. Szafrański, InterRidge global database of active submarine hydrothermal vent fields. Version 3.4. (2020).
69. R Core Team, R: The R Project for Statistical Computing (Version 4.2.3, R Foundation for Statistical Computing, Vienna, Austria, 2020).
70. C. Magneville *et al.*, mFD: An R package to compute and illustrate the multiple facets of functional diversity. *Ecography* **2022**, e05904 (2022).
71. S. Villéger, P. M. Novack-Gottshall, D. Mouillot, The multidimensionality of the niche reveals functional diversity changes in benthic marine biotas across geological time. *Ecol. Lett.* **14**, 561–568 (2011).
72. S. Villéger, G. Grenouillet, S. Brosse, Decomposing functional β-diversity reveals that low functional β-diversity is driven by low functional turnover in European fish assemblages. *Global Ecol. Biogeogr.* **22**, 671–681 (2013).
73. E. Maire, G. Grenouillet, S. Brosse, S. Villéger, How many dimensions are needed to accurately assess functional diversity? A pragmatic approach for assessing the quality of functional spaces *Global Ecol. Biogeogr.* **24**, 728–740 (2015).
74. A. Baselga, D. C. Orme, betapart: An R package for the study of beta diversity. *Methods in Ecol. Evol.* **3**, 808–812 (2012).
75. N. J. Gotelli, D. J. McCabe, Species co-occurrence: A meta-analysis of J. M. Diamond's assembly rules model. *Ecology* **83**, 2091–2096 (2002).
76. S. W. Kembel *et al.*, Picante: R tools for integrating phylogenies and ecology. *Bioinformatics* **26**, 1463–1464 (2010).
77. E. Laliberté, P. Legendre, A distance-based framework for measuring functional diversity from multiple traits. *Ecology* **91**, 299–305 (2010).